Don't Miss Weak Packets: Boosting LoRa Reception with Antenna Diversities

Ningning Hou, Xianjin Xia, Yuanqing Zheng
The Hong Kong Polytechnic University, Hong Kong, China
ningning.hou@connect.polyu.hk, {xianjin.xia, yqzheng}@polyu.edu.hk

***Abstract*—LoRa technology promises to connect billions of battery-powered devices over a long range for years. However, recent studies and industrial deployment find that LoRa suffers severe signal attenuation because of signal blockage in smart cities and long communication ranges in smart agriculture applications. As a result, weak LoRa packets cannot be correctly demodulated or even be detected in practice. To address this problem, this paper presents the design and implementation of MALoRa: a new LoRa reception scheme which aims to improve LoRa reception performance with antenna diversities. At a high level, MALoRa improves signal strength by reliably detecting and coherently combining weak signals received by multiple antennas of a gateway. MALoRa addresses a series of practical challenges, including reliable packet detection, symbol edge extraction, and phase-aligned constructive combining of weak signals. Experiment results show that MALoRa can effectively expand communication range, increase battery life of LoRa devices, and improve packet detection and demodulation performance especially in ultra-low SNR scenarios.**

I. Introduction

Low-Power Wide-Area Networks (LPWANs) such as LoRaWANs are promising technologies to connect billions of devices and enable large scale applications (*e.g.*, waste management, wildlife tracking, shipping and transportation scheduling, disaster rescue, *etc.*) [1–8]. LoRa adopts chirp spread spectrum (CSS) modulation in physical layer (PHY), which is resilient and robust to interference and noise. LoRa is expected to achieve up to 10 km communication range with battery-powered devices working for years. However, recent studies [9–13] find that the communication range of LoRa falls short of industry needs and expectations in real-world application scenarios. For example, LoRa devices deployed in urban environments or remote areas suffer severe signal attenuation due to signal blockage and long propagation distance. As a result, the Signal-to-Noise ratio (SNR) of LoRa packets can be severely degraded, leading to decoding failures at gateways and rapid battery drain of LoRa nodes. Suffering from low SNRs, weak packets of devices located deep inside buildings [14] may not even be detected, let alone decoded at nearby gateways separated by a number of concrete walls.

Current LoRaWAN adapts data rates in hopes of crossing an SNR threshold at minimum power consumption. However, some devices can still be out of reach even with the most conservative parameter settings. In this paper, we aim to improve the LoRa packet reception performance in ultra-low SNR scenarios without extra power consumption of battery-powered LoRa transmitters.

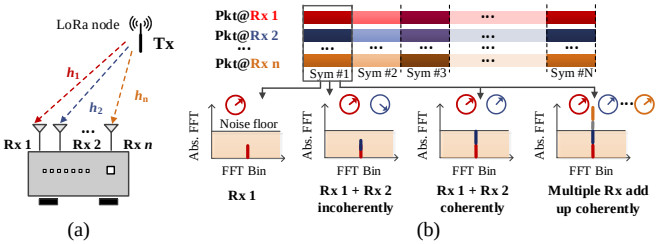

Fig. 1. Illustration of high level idea of MALoRa. (a) Multiple Rx antennas provide multiple phase-shifted signals of a packet, (b) Coherent combining of multiple antennas helps a gateway constructively add up the signals and improve SNR.

As illustrated in Fig. 1, we aim to leverage multiple antennas of a gateway to coherently combine the received signals from a LoRa transmitter so as to improve the packet reception performance. Although simple in concept, it entails tremendous technical challenges in the design and implementation of such a multi-antenna LoRa gateway. First, under ultra-low SNR scenarios, the received signals at each antenna can be very weak and submerged below the noise floor. In this case, the weak packets may not be detected. Second, in order to achieve coherent combining, the received signals should be aligned and constructively combined. Traditional channel sounding methods cannot be applied in the ultra-low SNR scenarios, since noise level could be too high for accurate channel measurement. Besides, the channel measurement could incur extra power consumption which cannot be afforded by battery-powered transmitters.

Current LoRa gateways detect the arrival of LoRa packets by detecting LoRa preambles, which consist of a few up-chirps. The preamble detection methods correlate an up-chirp with incoming signals and count the number of repetitive correlation peaks. A LoRa packet can thus be detected if multiple correlation peaks can be observed periodically. However, such methods do not work well in ultra-low SNR scenarios, since weak correlation peaks can be submerged below noise floors.

To improve the weak packet detection performance, we propose to fully leverage multiple up-chirps in LoRa preambles. While the energy of one chirp may be overwhelmed by noise, the energy of multiple chirps can be aggregated to improve the packet detection performance. Intuitively, we can combine multiple consecutive up-chirps by increasing the packet detection window size in a way that the energy of multiple up-chirps can add up constructively. However, if all

up-chirps are aggregated into one detection window, we cannot observe a certain number of periodic peaks anymore, which could lead to more false alarms. Fortunately, LoRa standard allows us to dynamically adapt and configure the preamble length of a LoRa packet before transmission. We configure the number of up-chirps in a LoRa preamble and the packet detection window to strike a balance between packet detection sensitivity and robustness.

Coherent combining has been extensively studied in wireless systems (*e.g.*, WiFi [15, 16], 5G [17]). Such works typically measure the wireless channels between a transmitter to multiple antennas, which involves high communication and computation overhead and require relatively good channel conditions to achieve accurate channel measurements. Besides, to reduce the power consumption of LoRa transmitters, the inter-packet interval of LoRa transmitters are much longer than those of other wireless systems (*e.g.*, WiFi, 5G), which make the channel measurement become easily obsolete and cannot be used for coherent combining.

To enable coherent combining of weak LoRa signals, we propose a novel phase difference measurement method that allows us to well-align phase-shifted copies of LoRa signals received at multiple antennas of a gateway. Unlike existing wireless channel measurement methods, we aim to accurately measure the phase differences between multiple wireless channels under ultra-low SNRs. To this end, we leverage the unique feature of LoRa to improve the phase difference measurement performance. Since LoRa preamble chirps share the same wireless channel as the payload chirps, we can exploit consecutive preamble chirps to accurately measure the phase shifts between wireless channels and compensate for payload chirps in coherent combining. As illustrated in Fig.1, once the phase differences can be accurately measured, we can coherently combine the phase-shifted copies of weak LoRa signals in a way that the SNR-enhanced LoRa signals can eventually cross the SNR threshold for successful packet reception.

We prototype MALoRa as a software-defined gateway with multiple synchronized USRPs. We evaluate MALoRa with commodity LoRa nodes in both indoor and outdoor environments. We comprehensively evaluate the performance of MALoRa in packet detection, symbol demodulation, SNR gain, and energy saving. Experiment results show that MALoRa can substantially improve packet detection and demodulation performance, and outperform the state-of-the-art benchmarks especially under ultra-low SNRs.

We summarize the key contributions as follows:

- We propose a novel technique that leverages the unique features of LoRa chirps and LoRa packet structure to improve the packet detection performance in ultra-low SNR environments.
- We propose a new phase difference measurement method that can be used to accurately measure phase differences between multiple wireless channels and coherently combine weak LoRa signals received by multiple antennas of a gateway.

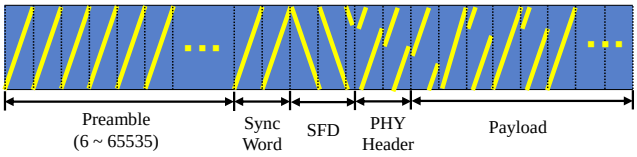

Fig. 2. LoRa packet structure. The preamble length is variable.

- We design and implement a prototype of MALoRa with software-defined radios and conduct comprehensive evaluations in various experiment settings. The experiment results with commodity LoRa nodes demonstrate that MALoRa can substantially improve weak packet reception performance especially under ultra-low SNR scenarios.

II. LoRa Primer

Chirp Spread Spectrum (CSS). LoRa adopts Chirp Spread Spectrum (CSS) modulation in physical layer. In CSS, a chirp signal sweeps through a bandwidth with an instant frequency increasing (up-chirp) or decreasing (down-chirp) linearly at a constant rate $k = \frac{BW^2}{2^{SF}}$, where SF represents the spreading factor. A *base chirp* sweeps from $-\frac{BW}{2}$ to $\frac{BW}{2}$ and can be represented as $C(t) = e^{j2\pi(\frac{k}{2}t - \frac{BW}{2})t}$. LoRa changes the initial frequency to modulate data with different symbols as follows

$$S(t, f_{sym}) = C(t) \cdot e^{j(2\pi f_{sym} t + \varphi_{sym})}, \quad (1)$$

where f_{sym} and φ_{sym} denote the initial frequency and initial phase of the chirp signal, respectively.

LoRa demodulation. A LoRa receiver demodulates a symbol by extracting the initial frequency of a LoRa chirp. We represent a received symbol with noise as below.

$$y(t) = h \cdot S(t, f_{sym}) + n(t), \quad (2)$$

where h denotes the wireless channel between a transmitter and a receiver and $n(t)$ represents noises. To demodulate a symbol, LoRa first *de-chirps* the received signal by multiplying with the *conjugate of base chirp* denoted as $C^{-1}(t)$ and then performs Fast Fourier Transform (FFT) to extract f_{sym}. This process can be represented as $Z(f) = FFT(y(t) \cdot C^{-1}(t))$. The FFT peak in $Z(f)$ indicates f_{sym} and its corresponding symbol.

LoRa packet structure. As illustrated in Fig. 2, a LoRa packet starts with a preamble which is composed of a varied number of base chirps, followed by two up-chirps as sync words, 2.25 down-chirps as a start frame delimiter (SFD) and the payload of the packet.

A LoRa receiver continuously monitors a channel to detect incoming packets. A receiver detects a LoRa packet by detecting the presence of LoRa preamble. When a preamble is detected, it further detects SFD and extracts frame timing information from preamble and SFD chirps to demodulate symbols in the payload of the packet.

III. Motivation

Target application scenario. LoRa is promising to connect low-power IoT devices in a wide area thanks to its large

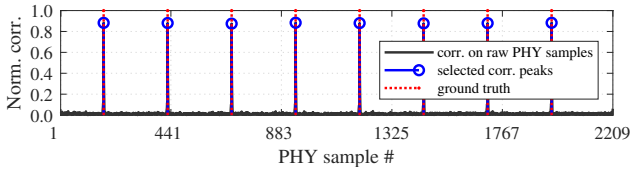

(a) Correlation results with high SNR

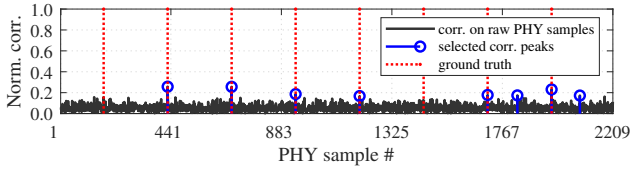

(b) Correlation results with low SNR

Fig. 3. Preamble correlation results for LoRa packet detection: (a) SNR = 0 dB; (b) SNR = -25 dB.

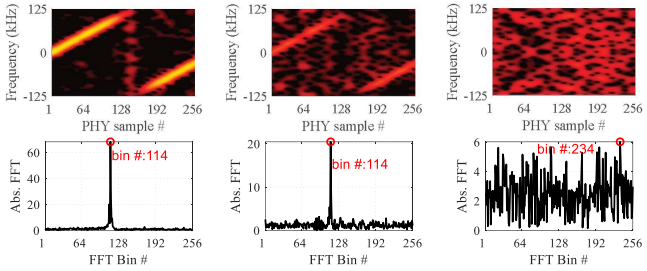

(a) SNR = 0 dB (b) SNR = -15 dB (c) SNR = -30 dB

Fig. 4. Spectrogram and de-chirp FFT results of one chirp under different SNRs. The energy peak of a chirp is submerged by noise under ultra-low SNR.

link budget and high sensitivity of LoRa receiver radios. Commodity radio manufacturers advertise that LoRa radios can decode a packet over a long communication range even when the signal strength falls below noise floors. However, recent studies [11, 18] find that the communication range of LoRa can be much shorter in urban environments due to dramatic power losses because of signal blockage and signal attenuation over long communication ranges. In this case, a commodity receiver can barely receive any packets from a LoRa node. This problem prohibits the wide adoption of LoRa technology in smart city applications, where reliable data collection is essential yet challenging. Our work aims to fill this gap by supporting LoRa communications in such challenging environments with ultra-low SNRs. We believe improving the weak packet reception performance is critical to many real-world usage scenarios such as wild fire detection in remote field and intrusion detection in smart building which need infrequent but reliable data transfer – where weak packets should not be missed.

Problem with low-SNR LoRa reception. A LoRa radio requires a minimum SNR to correctly detect and receive a packet. If the SNR of a packet falls below the minimum requirement, the packet cannot be received. In the following, we empirically study the LoRa packet reception process and elaborate why it is challenging to receive a LoRa packet when SNR is low.

LoRa packet reception generally involves two key phases: 1) packet detection and 2) payload demodulation. Commodity LoRa radios detect packets with Channel Activity Detection (CAD) operation which detects LoRa preamble by correlating incoming signals with standard base chirps. Fig. 3(a) and (b) compare preamble detection results in high and low SNRs. When SNR is high as presented in Fig. 3(a), we observe periodic correlation peaks. A receiver can thus count the number of correlation peaks and detect incoming packets. However, when SNR decreases as shown in Fig. 3(b), the correlation peaks drop dramatically and mess up with noise peaks. If SNR further decreases, current packet detection method may not even be able to detect any correlation peaks and separate them from noises. As such, conventional packet detection method fails in low SNR scenarios. If a packet cannot be detected due to low SNR in the packet detection phase, the LoRa receiver will skip the payload demodulation phase as if there were no incoming packet.

If a packet with sufficient SNR can be successfully detected, its payload chirps will be captured for symbol demodulation. Fig. 4 examines the impacts of SNRs on symbol demodulation. Normally, we can correctly demodulate a symbol from the FFT results if SNR is sufficiently high. As shown in Fig. 4(a), when SNR is $0\,\mathrm{dB}$ (a typical LoRaWAN scenario in short range), the conventional symbol demodulation method (*i.e.*, multiplying with a down chirp and performing FFT) can detect the FFT peak and accomplish the demodulation task. Even when the SNR decreases below the noise floor such as $-15\,\mathrm{dB}$ (a long range or wall penetrating scenario), the conventional demodulation method can sometimes work since the power of a LoRa chirp can be concentrated into a single FFT bin by multiplying with a down chirp as shown in Fig. 4(b). As a result, we can still correctly demodulate the received symbol whose the initial frequency correspond to bin # 114 in the experiments. However, when SNR further decreases to $-30\,\mathrm{dB}$ (ultra-low SNR scenario because of blockage of line-of-sight path or signal attenuation over a longer range), the conventional demodulation method cannot find the correct FFT peak any more, which leads to symbol errors in the demodulation phase.

Note that coding schemes (*e.g.*, Hamming code, Gray code) are adopted in LoRa physical layer which are capable of correcting a small number of symbol errors (*e.g.*, due to carrier frequency offsets). Such coding schemes however cannot save weak packets in such ultra-low SNR scenarios, since all payload chirps suffer high noises and excessive symbol errors. Similarly, retransmission could not help either, since the channel conditions would remain poor in ultra-low SNR scenarios. As a result, weak packets with low SNRs are more likely to be missed in both packet detection and payload demodulation phases.

Opportunity. Latest commodity gateways are equipped with multiple antennas. In downlink transmissions (*i.e.*, from a

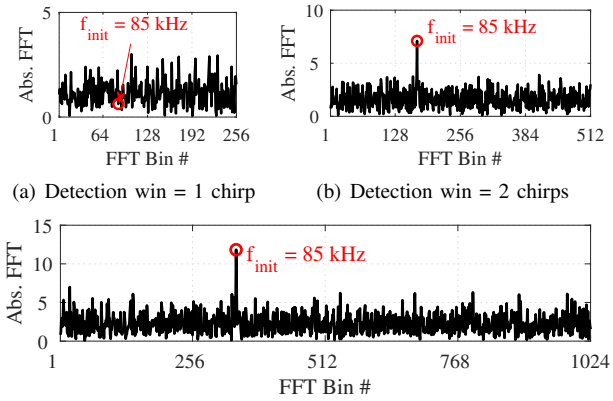

(a) Detection win = 1 chirp (b) Detection win = 2 chirps

(c) Detection win = 4 chirps

Fig. 5. Packet detection with different lengths of detection windows: the larger the detection window, the higher the energy peak of the targeted chirp signal. We can increase detection window length to detect a packet in ultra-low SNR scenarios.

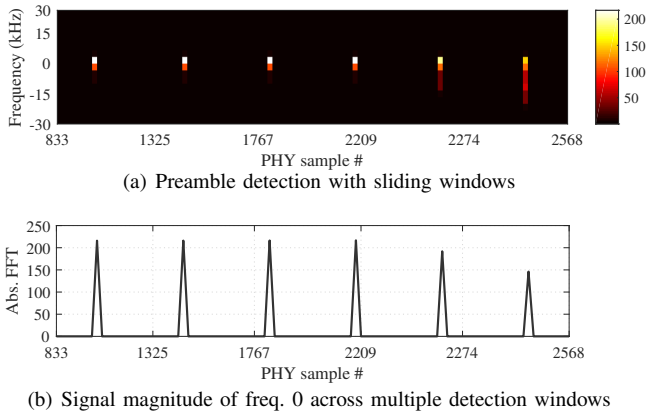

(a) Preamble detection with sliding windows

(b) Signal magnitude of freq. 0 across multiple detection windows

Fig. 6. Packet detection with a detection window in length of 4 chirps.

gateway to LoRa nodes), multiple antennas are used to transmit different messages to different LoRa nodes. To support concurrent downlink transmission, the antennas are configured with orthogonal parameters (*e.g.*, different channels, SFs). As such, the downlink transmissions can happen without any collisions to LoRa nodes. In uplink reception, the multiple antennas work independently in packet detection and demodulation.

In this paper, we aim to fully leverage the multiple antennas of a gateway to improve the LoRa packet reception performance in ultra-low SNR scenarios. Intuitively, we propose novel techniques to add up the weak signals of multiple antennas and strengthen LoRa signals. Even if the signal SNRs may fall below SNR threshold of an individual antenna, we can still combine signals of multiple antennas to pull up SNRs above the threshold for correct packet demodulation. The more antennas we use, the higher SNR gains we may achieve.

IV. Design Details

A. Packet Detection with Chirp Combination

The standard correlation based method (*e.g.*, CAD of a LoRa radio) fails to detect weak packets in ultra-low SNRs as shown in Fig. 3(b). In this subsection, we present a new method for weak LoRa packet detection in ultra-low SNRs.

We exploit the fact that a LoRa preamble consists of consecutive identical base chirps, which means that the dechirped signals of any preamble chirps would have the same frequency. When we perform FFT on the dechirped signals of a preamble chirp, the magnitude of FFT peak corresponds to the accumulated energy of all samples of the chirp. If more samples from a longer signal duration (*e.g.*, N preamble chirps) are put into an FFT, a higher FFT peak can be expected because the energy of samples from N chirps coherently add up in one FFT bin. This motivates us to increase the length of detection window from one chirp to N chirps to detect a weak LoRa preamble.

Fig. 5 shows the FFT results of dechirped signals of a weak preamble with different detection window sizes. We observe that though the energy of a single preamble chirp is submerged below noise floor as shown in Fig. 5(a), the FFT peak of the dechirped preamble signals becomes higher as the detection window size increases from one chirp to four chirps as shown in Fig. 5(b). As more preamble signals are used for FFT analysis, more signal energy accumulates and the resulting FFT peak grows higher. In contrast, the noise floor remains at almost the same level during the process because noise power will not accumulate in anyone of the FFT bins due to the randomness of noises. As a result, the energy of preamble signals (*i.e.*, FFT magnitude) would gradually increase to surpass noise floor as more chirps are added into a detection window, as shown in Fig. 5(b,c).

In practice, we use a sufficiently long detection window that accumulates the signal energy of N chirps to detect a weak LoRa preamble. To avoid false alarms, we slide a detection window across received signals. If the FFT peaks can be periodically detected multiple times in the same FFT bin when we slide the detection window to different offsets, we can then assure that a real LoRa preamble is present. To achieve real-time packet detection, MALoRa slides the detection window with a large offset per step. We empirically configure the sliding offset as one chirp duration per step in our implementation. It can effectively reduce computation overhead without missing most packets.

Fig. 6 presents the detection results of a weak LoRa preamble (SNR=-25 dB) using a detection window in length of 4 chirps (*i.e.*, $N = 4$). As we slide the detection window across the signals of the preamble, periodic high energy peaks are detected in the same frequency bin (*e.g.*, $f = 0$) across different offset positions as shown in Fig. 6(a). We plot the magnitude of the detected frequency (*i.e.*, $f = 0$) in Fig. 6(b). We see that the gap between detected peaks equals to the length of a chirp duration. This periodic appearance of frequency peaks indicates the presence of a LoRa preamble.

B. Packet Demodulation with Multiple Antennas

Though we can combine multiple preamble chirps to detect a weak LoRa packet, the same method cannot be used to decode the packet because chirps in the payload usually differ

from each other. Instead, MALoRa coherently combines the signals of multiple antennas and leverages the SNR gains to demodulate and decode a weak packet. In the following, we first present how to measure channel difference between a transmitter to multiple antennas.

Measuring channel difference. Intuitively, we may extract channel h from a received LoRa symbol $y(t)$ according to Eq.(2). We can first dechirp $y(t)$ and then extract the phase of channel from the FFT response of the demodulated symbol.

However, the raw phase measurement may contain not only channel phase, but also phase distortions incurred by radio hardware such as Carrier Frequency Offset (CFO) and Sampling Timing Offset (STO). We cannot use existing methods to estimate and calibrate for those phase distortions because it is not likely to estimate the correct CFO and STO in ultra-low SNRs. Without loss of generality, we take the phase distortions of radio hardware into account and update the received signals of a LoRa symbol (*i.e.*, Eq.(2)) as below.

$$y(t) = h \cdot e^{j\varphi_{distort}(t)} \cdot S(t, f_{sym}) + n(t), \tag{3}$$

where $\varphi_{distort}(t)$ characterizes the phase distortions of radios including CFO, STO and phase jitters caused by hardware imperfection [4].

MALoRa uses two synchronized Rx antennas of a gateway to calibrate phase distortions in received low-SNR signals. Let $y_1(t)$ and $y_2(t)$ denote the signal copies received by two antennas. As the two antennas are synchronized in time, frequency and phase, $y_1(t)$ and $y_2(t)$ would have the same CFO, STO as well as the resulting phase distortions $\varphi_{distort}(t)$. Then, we can remove $\varphi_{distort}(t)$ by multiplying $y_1(t)$ with the conjugate of $y_2(t)$ denoted as $y_2^*(t)$, which is represented as follows.

$$y_1(t) \cdot y_2^*(t) = h_1 \cdot h_2^* + \widetilde{n}(t), \tag{4}$$

where $\widetilde{n}(t)$ denotes noises after conjugate multiplication. The phase of $h_1 \cdot h_2^*$ corresponds to the phase difference between channels h_1 and h_2, *i.e.*, $\Phi(h_1 \cdot h_2^*) = \Phi(h_1) - \Phi(h_2)$, where $\Phi(\cdot)$ extracts the phase of a complex number.

Ideally, we can use Eq.(4) to directly measure the phase difference between $y_1(t)$ and $y_2(t)$ for coherent combining. However, in the case of ultra-low SNRs, the power strength of noises can be comparable with or even higher than the power of signals. As a result, $h_1 \cdot h_2^*$ may be submerged below noise floor and the phase measurement of $h_1 \cdot h_2^*$ would be distorted by $\widetilde{n}(t)$ in practice.

MALoRa pulls up SNRs of signal component $h_1 \cdot h_2^*$ by leveraging multiple chirps in LoRa preamble. Basically, as chirps in preamble are identical, we can use Eq.(4) to extract the same $h_1 \cdot h_2^*$ from any preamble chirps of the two antennas. Although the signal energy of $h_1 \cdot h_2^*$ from a single chirp is submerged below the noise floor as shown in Fig. 8(b), we can aggregate the signals (*i.e.*, $h_1 \cdot h_2^*$) extracted from multiple preamble chirps to accumulate signal energy in one FFT bin. Fig. 8(c) shows the FFT results when 8 preamble chirps are added up constructively, where the peak at bin #1 corresponds to $h_1 \cdot h_2^*$. Comparing Fig. 8(b) and Fig. 8(c), we see that

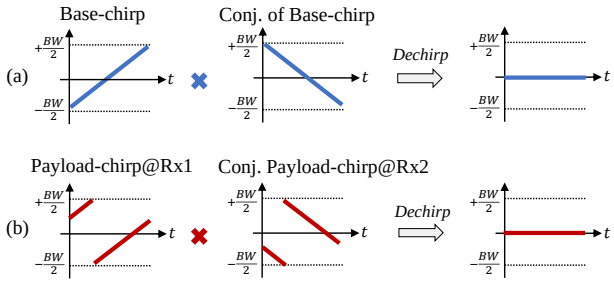

Fig. 7. Conjugate multiplication removes differences in base-band chirp signals. (a) Dechirp a standard preamble chirp, (b) Dechirp a payload-chirp with Rx pairs by multiplying the chirp received by Rx1 with the conjugate of the signal copy received by Rx2.

the FFT peak of component $h_1 \cdot h_2^*$ emerges above the noise floor as the signal energy of $h_1 \cdot h_2^*$ from all preamble chirps accumulates in bin #1. Then we can accurately measure the phase of the emerging FFT peak representing $h_1 \cdot h_2^*$.

Since LoRa chirps of the same packet pass through the same wireless channel, we find that the same channel component ($h_1 \cdot h_2^*$) can also be obtained from other parts of a packet (*e.g.*, sync words, SFD and payload) in addition to preamble. Although chirps in other parts usually differ from each other and the preamble chirps (*e.g.*, initial frequency), the difference of chirps can be removed by Eq.(4). Since $y_1(t)$ and $y_2(t)$ in Eq.(4) correspond to the same symbol received by two antennas, they share the same base-band chirp signal (*i.e.*, $S(t, f_{sym})$). This chirp signal is removed during the process of conjugate multiplication (*i.e.*, $y_1(t) \cdot y_2^*(t)$). As illustrated in Fig. 7, the conjugate multiplication would produce the same results for both a preamble chirp and a payload symbol. The results produced by Eq.(4) (*i.e.*, $h_1 \cdot h_2^*$) are indeed chirp independent. The same channel component ($h_1 \cdot h_2^*$) can be extracted from different parts of the same packet (*e.g.*, preamble and payload). As such, the signal components ($h_1 \cdot h_2^*$) extracted from different parts of the packet can be added up constructively to strengthen the signal energy of $h_1 \cdot h_2^*$. If chirps from both preamble and payload of a packet are aggregated to enhance SNRs for signal ($h_1 \cdot h_2^*$), we can expect to have sufficiently high signal energy to accurately measure the channel difference of two antennas.

Fig. 8 presents the results of channel difference measurement from signals of a LoRa packet (SNR = -25 dB) received by two antennas. We see from Fig. 8(a) that the signals (*i.e.*, $h_1 \cdot h_2^*$) extracted from preamble, SFD and payload form a long horizontal line, indicating that the extracted signals have the same frequency (*i.e.*, $f = 0$). As shown in Fig. 8(b), the signal strength of ($h_1 \cdot h_2^*$) extracted from a single chirp is below the noise floor, from which we cannot correctly measure the channel difference of the two antennas. When 8 preamble chirps are aggregated together, the accumulated signal energy of $h_1 \cdot h_2^*$ increases above the noise floor as shown in Fig. 8(c). Finally, when more chirps from both preamble and payload are aggregated, the FFT peak of $h_1 \cdot h_2^*$ grows higher as shown in Fig. 8(d), from which the phase difference between channels

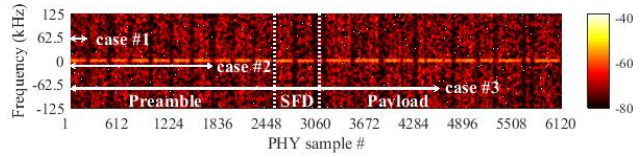

(a) Spectrum of the conjugate multiplication results of two Rx antennas

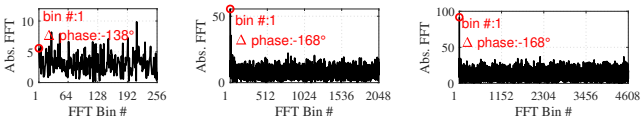

(b) Case #1 (c) Case #2 (d) Case #3

Fig. 8. Measuring channel difference with two synchronized antennas. (a) spectrum of the conjugate multiplication results of an Rx pair: the energy of all chirps concentrates at zero frequency; (b-d) measuring channel difference with 1 preamble chirp (case #1), 8 preamble chirps (case #2), and 16 different kinds of chirps including preamble, SFD and payload chirps (case #3), respectively.

h_1 and h_2 can be measured more reliably.

Coherent combining. After measuring the channel difference between any two antennas, we next combine multiple antennas to obtain SNR-enhanced signals.

Let $y_i(t)$ denote the received signals of the i^{th} antenna and $\Delta\phi_{ij}$ denote the phase difference between signals of the i^{th} and the j^{th} antennas. MALoRa compensates phase differences among signals of different antennas for coherent combining. The signal combination of M antennas is represented as below.

$$Y_{combine}(t) = y_1(t) + \sum_{i=2}^{M} y_i(t) \cdot e^{-j\Delta\phi_{i1}}, \tag{5}$$

where $y_i(t) \cdot e^{-j\Delta\phi_{i1}}$ rotates the phase of $y_i(t)$ to align with the signals of the first antenna. After combining the weak signals of multiple antennas, MALoRa will feed the obtained SNR-enhanced signals (*i.e.*, $Y_{combine}(t)$) into a standard LoRa demodulation and decoding pipeline for symbol demodulation and payload data extraction.

Fig.9 presents the results of coherent combining with different numbers of antennas. Fig.9(a) shows the signals of a weak LoRa symbol before coherent combining and signal strength enhancement. The symbol cannot be demodulated due to ultra-low SNRs. As the weak signals of more antennas are added constructively, we observe the LoRa chirp starts to emerge in the spectrogram shown in Fig.9(b) when we combine the signals received by 4 antennas, and become clearer when we combine the signals of 8 antennas in Fig.9(c). Accordingly, the FFT magnitude of the demodulated frequency becomes higher as more antennas are combined. Finally, the symbol of a weak packet can be correctly demodulated with the combined signals of multiple antennas.

C. Integration with LoRaWAN

MALoRa relies on the accumulated signal energy of multiple preamble chirps to detect weak LoRa packets. Commodity LoRa radios (*e.g.*, Semtech SX1276) support a maximum preamble length of 65535 chirps. Though a longer preamble is beneficial for detecting more packets with lower SNRs, an

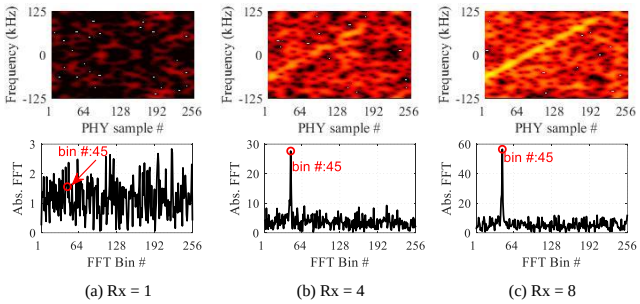

(a) Rx = 1 (b) Rx = 4 (c) Rx = 8

Fig. 9. Coherent combining with different number of antennas (SNR = -30 dB). (a) Standard LoRa demodulation without combining, (b) combine with 4 antennas, and (c) combine with 8 antennas.

excessively long preamble would incur high communication overhead and consume more energy for LoRa nodes. More importantly, a long preamble may not directly translate to higher gains for packet decoding, because the SNR gain is limited by the number of antennas in coherent combining.

Assume that a gateway has N_{ant} antennas and a packet is received with the same power strength by all antennas. As MALoRa combines the signals of N_{ant} antennas for packet decoding, we can expect approximately $N_{ant}\times$ increase of signal strength in comparison with the raw signals of a single antenna. Similarly, the signal strength is expected to increase by $N\times$ if we combine N preamble chirps together in a detection window for packet detection.

In particular, if $N < N_{ant}$, it may lead to miss detection of packets; if $N \gg N_{ant}$, a LoRa node will then suffer energy waste due to transmitting of an overlong preamble. We basically requires $N \approx N_{ant}$ to ensure that any detected packet would finally get decoded. Then, we can coarsely estimate the length of preamble (N_{pre}) as below.

$$N_{pre} = (n_{win} - 1) + N_{ant}, \tag{6}$$

where n_{win} denotes the number of sliding windows used for preamble detection.

MALoRa employs an adaptive preamble strategy to balance between communication performance and overhead. A LoRa node can coordinate with a gateway to negotiate on the change of preamble length. Specifically, the initial configuration of preamble length is calculated according to Eq.(6), which can be performed when the node first joins a LoRaWAN network. The node can adjust preamble length to adapt to new network conditions. In current implementation, the preamble length of each LoRa node is empirically configured to strike a balance between reception performance and communication overhead. In the future, we plan to optimize the parameter configuration by jointly considering channel dynamics, battery life, and decoding capabilities of gateway.

V. Evaluation

A. Methodology

Gateway. We build a LoRa gateway (Fig. 10) using synchronized USRP SDRs (N210) based on the gr-lora open-source project [19]. The USRPs are synchronized with an

Fig. 10. Implementation.

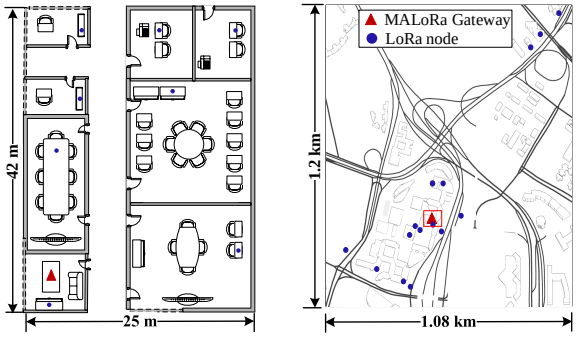

(a) Indoor layout (b) Outdoor layout

Fig. 11. Testbed settings of MALoRa.

external clock source (CDA-2990) and PHY samples are collected and processed using a laptop through a 100 Gigabit Ethernet Switch. In practice, a multi-antenna gateway can be built using low-cost components similar to multi-antenna access points [16, 20].

LoRa nodes. We use commodity LoRa nodes (Fig. 10) as transmitters, composed of Dragino LoRa shields [21] and Semtech SX1276 radios. We use Arduino Uno boards to set key parameters of LoRa nodes. We set the default central frequency, bandwidth (BW), spreading factor (SF), coding rate (CR), and transmission power of LoRa communication as 915 MHz, 250 kHz, 8 , $4/8$, and 23 dBm, respectively.

Experiment setup. We evaluate MALoRa in a university and neighborhoods spanning $1.08\,\mathrm{km} \times 1.2\,\mathrm{km}$. The testbed consists of 40 LoRa nodes and a multi-antenna gateway. We place our gateway in one meeting room (Fig. 11 (a)) inside a building and put LoRa nodes in both indoor and outdoor environments (Fig. 11 (b)). We configure each node to transmit 50 packets and we conduct experiments with a total number of 2000 measurements.

Metrics. We evaluate the performance of MALoRa with three key metrics: (1) *Symbol Error Rate (SER)*, (2) *Packet Reception Ratio (PRR)*, and (3) *Goodput*. We also evaluate the energy consumption of LoRa nodes.

Benchmarks. We conduct comprehensive evaluation and compare the performance against the following benchmarks: (1) *LoRaWAN* — a standard LoRa packet decoder [19]; (2) *Charm* [11] — a distributed LoRa coherent combining scheme. Note that the standard LoRa packet decoder (*i.e.*, LoRaWAN) does not use multi-antenna. For fair comparison, we decode

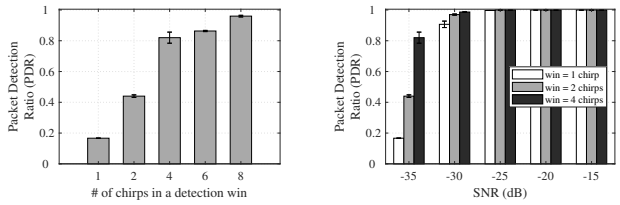

(a) (b)

Fig. 12. Packet detection performance of MALoRa: (a) with different length of packet detection window (SNR=-35 dB), and (b) under different SNRs.

signals of each Rx antenna and select the best decoding results as the final results for the standard LoRaWAN.

B. Packet Detection Performance

This experiment evaluates the performance of weak packet detection. We setup 10 LoRa nodes and one gateway in an indoor environment. The gateway receives the raw signals of packets transmitted by the LoRa nodes. To evaluate the performance of packet detection in a range of different SNRs, we use the gateway to record background noises and add up received noises and packet signals to synthesize signals with various SNR conditions. We then run MALoRa to detect packets from the synthesized low-SNR signals.

Fig. 12(a) presents the packet detection results of MALoRa using different packet detection window size when SNR = -35 dB. Packet detection with a single chirp represents the approach used by a standard LoRa receiver. As expected, more than $80\,\%$ packets are missed by the standard LoRa packet detection method when SNR is -35 dB. In contrast, the packet detection performance is improved dramatically by MALoRa as it aggregates the power of multiple chirps for packet detection. As more chirps are combined in a detection window, the packet detection ratio increases accordingly. For example, more than $82\,\%$ packets are detected when we use 4 chirps in a detection window, meaning that only $18\,\%$ of weak packets were missed. The packet detection ratio further increases to $96\,\%$ as the length of detection window increases to 8 chirps.

Fig. 12(b) evaluates packet detection performance under different SNR conditions. We see that the standard LoRa packet detector (*i.e.*, win=1 chirp) can still reliably detect packets when SNR is as low as -25 dB. When SNRs further decreases below -30 dB, however, the packet detection ratio starts to drop dramatically. In contrast, MALoRa still performs well when using 4 chirps and 8 chirps for packet detection. The more chirps combined in a detection window, the more packets can MALoRa detect.

C. Packet Decoding Performance

In this subsection, we focus on the packet demodulation performance of MALoRa and evaluate the impacts of various factors. The experiments were conducted both indoors and outdoors. We use 40 LoRa nodes and a gateway with up to 8 Rx antennas. In order to evaluate the demodulation performance with low SNRs, we deploy LoRa nodes far away

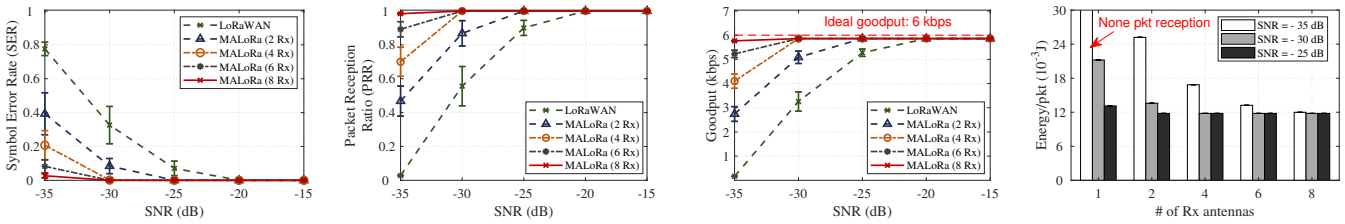

(a) Symbol Error Rate (b) Packet Reception Ratio (c) Goodput (d) Energy consumption

Fig. 13. Packet decoding and energy performance of MALoRa under different SNRs and different numbers of antennas.

from the gateway and also deeply inside a building, separating the nodes from the gateway by a number of concrete walls. The gateway collects PHY samples when commodity LoRa nodes transmit packets in different locations. We run MALoRa to detect and demodulate packets with different SNR conditions.

Decoding performance. Fig. 13 presents the decoding performance of MALoRa in different SNRs. The results of 1 Rx correspond to a standard LoRa decoder without assistant of multiple antennas, which is displayed as a baseline for performance evaluation of MALoRa. We see that the standard LoRaWAN method can correctly demodulate packets when SNRs are as low as $-20\,\mathrm{dB}$. As shown in Fig. 13(a), the symbol error rates increase as SNRs decrease from $-25\,\mathrm{dB}$ to $-35\,\mathrm{dB}$. In particular, when SNR is $-35\,\mathrm{dB}$, $80\,\%$ of the symbols are incorrectly demodulated. Such symbol errors cannot be corrected by the error correcting schemes adopted by LoRa standard, resulting in a packet reception ratio of nearly 0 as shown in Fig. 13(b).

In contrast to the high symbol error rates of the standard LoRaWAN decoder (*i.e.*, 1 Rx), more symbols can be correctly demodulated by MALoRa even when SNRs drop below $-25\,\mathrm{dB}$. Moreover, the symbol error rates of MALoRa can be reduced as we coherently combine more antennas of the gateway. As shown in Fig. 13(a) and (b), when MALoRa combines 8 Rx antennas, the symbol error rate is retained below $5\,\%$ and almost all packets are received since the small number of symbol errors can be corrected by the error correcting codes. In comparison with the standard LoRaWAN decoder, MALoRa (8 Rx) produces an SNR gain of about $10\,\mathrm{dB}$, which can effectively translate to longer communication ranges as well as longer battery life for LoRa nodes in practice.

Fig. 13(c) evaluates the goodput of MALoRa under different SNRs. As expected, the goodput of the standard decoder decreases from $6\,\mathrm{kbps}$ to nearly $0\,\mathrm{kbps}$ as the SNR decreases to $-35\,\mathrm{dB}$. The goodputs of MALoRa with 2, 4 and 6 antennas exhibit a similar trend. As more antennas are combined, higher goodputs are produced when SNR $< -20\,\mathrm{dB}$. The goodput of MALoRa with 8 Rx approaches to the maximum possible goodput in all SNR conditions, since almost all transmitted symbols can be corrected demodulated.

Energy performance. In the following, we evaluate the energy performance of MALoRa. To this end, we transmit a sequence of identical packets using a LoRa node and record the received PHY samples with multiple antennas of a gateway. We consider a simplified scenario where a packet will be retransmitted if it cannot be decoded correctly. On the other hand, if a packet can be correctly decoded, we consider the next packet as a new packet. We calculate the average energy consumption of transmitting a packet based on the datasheet of Semtech SX1276 [2] and report the energy consumption per packet transmission in Fig. 13(d).

As expected, a node generally consumes less energy to transmit a packet in higher SNRs when the same number of antennas are used for packet decoding. Under the same SNR conditions, the per-packet energy consumption decreases as more antennas are used in coherent combining. Take the case of SNR = $-35\,\mathrm{dB}$ as an example. The per-packet energy consumption is $25\,\mathrm{mJ}$ when MALoRa uses 2 antennas for packet decoding. The energy consumption decreases to $11\,\mathrm{mJ}$ as the number of antennas increases to 8, resulting in $56\,\%$ energy savings. When the channel condition is good (*e.g.*, SNR = $-25\,\mathrm{dB}$), the marginal gain of using more antennas decreases, since almost all packets can be correctly decoded with fewer antennas already.

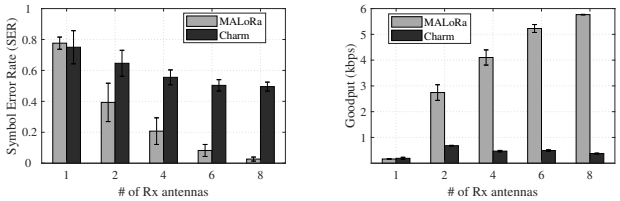

(a) Symbol Error Rate (SER) (b) Goodput

Fig. 14. Performance comparison with state-of-the-art: (a) Symbol error rate; and (b) Goodput.

Comparison against the state-of-the-art. In this experiment, we compare the performance of MALoRa and Charm in decoding the same packets when SNR = $-35\,\mathrm{dB}$. In Fig. 14, we see that the SERs of MALoRa and Charm remain at the same level when multi-antenna is not used (*i.e.*, 1 Rx). As the number of antennas increases to 8, the SER of MALoRa decreases to $4\,\%$, whereas the SER of Charm is still as high as $56\,\%$ when 8 antennas are used. When SNR is low, we find that Charm cannot reliably estimate and calibrate frequency and timing offsets among multiple distributed antennas. Moreover, as the clocks of distributed antennas drift differently, it is extremely difficult to compensate for the frequency drifts during packet transmissions. As a result, the signals received

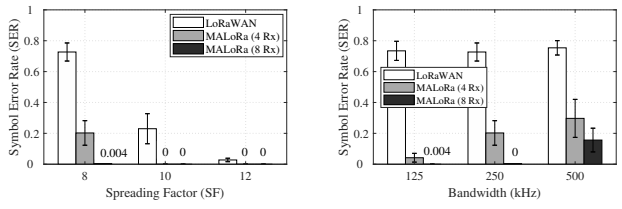

Fig. 15. Impact of LoRa packet configuration (SNR = $-35\,\mathrm{dB}$): (a) Spreading factor and (b) Bandwidth.

by multiple distributed antennas cannot be aligned and sometimes suffer destructive combining, which substantially affect symbol demodulation performance.

Moreover, as a packet with high SERs (*e.g.*, $>20\,\%$) cannot be correctly received, the goodput of Charm remains lower than $1\,\mathrm{kbps}$ as shown in Fig. 14(b). In contrast, the goodput of MALoRa increases almost linearly up to $5.8\,\mathrm{kbps}$ as the number of antennas increases from 1 to 8.

Impact of packet configuration. This experiment examines the impact of LoRa packet configuration on MALoRa performance when SNR = $-35\,\mathrm{dB}$.

We first vary Spreading Factor (SF) of LoRa packets from 8 to 12. Experiment results are shown in Fig.15(a). Generally, MALoRa performs better with larger SF. This result is consistent with the performance of a standard LoRa decoder. We notice that MALoRa with more Rx antennas can achieve more accurate decoding result when SF is small. For example, when SF = 8, the standard LoRa packet decoder (*i.e.*, 1 Rx) has SER of $72\,\%$, while MALoRa with 4 Rx antennas achieves SER of $20.3\,\%$ and MALoRa with 8 Rx antennas further improves the decoding accuracy with SER of $0.4\,\%$. This experiment results indicate that a LoRa node can select a small SF to save energy when a gateway is equipped with multiple Rx antennas.

We then vary Bandwidth of LoRa packets. Specifically, we evaluate MALoRa with BW = $125\,\mathrm{kHz}$, $250\,\mathrm{kHz}$, and $500\,\mathrm{kHz}$, respectively. Fig.15 (b) represents the results. We observe that MALoRa performs better with smaller bandwidth and more Rx antennas can help decrease the symbol error rate. An interesting observation is that in ultra-low SNR scenarios (SNR = $-35\,\mathrm{dB}$), increasing bandwidth will not improve the demodulation performance. This is because the energy of one LoRa chirp is limited and spread across a certain frequency band. As the bandwidth increases, the energy of noise within that frequency band also increases. Therefore, when SNR is extremely low, packets with larger bandwidth become even harder to be decoded correctly.

VI. Related Work

Recent years have witnessed substantial advances in LoRa technology such as performance measurement and optimization [22, 23], media assess control [24, 25], concurrent transmissions [3, 26–30], and LoRa backscatter [31].

Latest advances in LoRa communication range enhancement [11, 12, 18, 32] exploit multiple distributed gateways and joint decode at a centralized cloud server. For example, Charm [11] designs a coherent decoder which aggregates raw physical layer samples of multiple distributed gateways and try to coherently combine them to boost the SNRs of LoRa signals. Chime [12] uses multiple gateways to estimate the optimal operating frequency for signal strength improvement and power consumption reduction. OPR [18] collect the link layer information across multiple gateways to a centralized cloud server and corrects corrupted bits. Although these approaches can achieve better performance than an individual gateway, they typically require sample-level time-synchronization among distributed gateways, which is extremely hard to achieve in practice for commodity LoRa gateways. Besides, various factors influence the performance of coherent combining such as CFOs and STOs across distributed gateways [26]. Moreover, these approaches incur high network traffic since a large volume of raw physical layer samples need to be transmitted to a centralized server.

Our work is related to the single input multiple output technology in information theory [17, 33] in which multiple antennas at the receiver are used to improve packet reception performance. Such works typically require accurate channel measurements to align the signals which is hard to achieve for LoRa especially when wireless channel condition is poor. In this paper, we overcome a series of practical challenges (*e.g.*, packet detection in low SNR, coherent combining without active channel measurement).

Recent works aim to support concurrent transmissions for LoRa [30, 34–38]. Choir [26] aims to support LoRa concurrent transmissions by exploiting the frequency offsets introduced by LoRa hardware. FTrack [3] leverages the time misalignment of LoRa chirps to resolve LoRa collisions. While PCube [39] uses wireless channel phase information to separate collided symbols. NScale [36] amplifies the time offsets between colliding packets with non-stationary signal scaling. Our work is orthogonal to these works in that it improves packet detection and coherently combines weak LoRa packets, which can help these concurrent transmission schemes to better recover packet collisions in low SNR scenarios.

VII. Conclusion

This paper presents the design and implementation of MALoRa which improves LoRa packet reception performance in low SNR scenarios. MALoRa overcomes a series of practical challenges in achieving coherent combining of multiple antennas of a gateway. In particular, MALoRa proposes a new packet detection method that fully leverages long preambles of LoRa packets so that weak packets can still be detected and thus combined in the following demodulation phase. MALoRa proposes a phase-aligned coherent combining method that ensures constructive combining of LoRa signals received at multiple antennas. Our experiment results show that the collocated antennas of a gateway can still provide sufficient spatial diversity that can be harvested to boost weak LoRa packet reception performance.

ACKNOWLEDGEMENTS

This work is supported in part by Hong Kong General Research Fund (GRF) under grant PolyU 152165/19E, in part by the Start-up Fund for Research Assistant Professor (RAP) under the Strategic Hiring Scheme of Hong Kong PolyU under grant P0036217, and in part by the National Nature Science Foundation of China (NSFC) under Grant No. 62102336. Yuanqing Zheng is the corresponding author.

REFERENCES

[1] LoRa Alliance, "LoRaWAN for Developer," in *https://lora-alliance.org/lorawan-for-developers*, Aug. 2020.

[2] Semtech, "Semtech SX1276: 137MHz to 1020MHz long range low power transceiver," in *https://www.semtech. com/products/wireless-rf/lora-transceivers/sx1276*, Aug. 2020.

[3] X. Xia, Y. Zheng, and T. Gu, "Ftrack: Parallel decoding for lora transmissions," *IEEE/ACM Transactions on Networking*, vol. 28, no. 6, pp. 2573–2586, 2020.

[4] X. Xia, Y. Zheng, and T. Gu, "LiteNap: Downclocking LoRa Reception," in *IEEE INFOCOM 2020 - IEEE Conference on Computer Communications*, 2020, p. 2321–2330.

[5] Y. Peng, L. Shangguan, Y. Hu, Y. Qian, X. Lin, X. Chen, D. Fang, and K. Jamieson, "Plora: A passive long-range data network from ambient lora transmissions," in *Proceedings of the 2018 Conference of the ACM Special Interest Group on Data Communication*, 2018, pp. 147–160.

[6] N. Hou and Y. Zheng, "Cloaklora: A covert channel over lora phy," in *2020 IEEE 28th International Conference on Network Protocols (ICNP)*. IEEE, 2020, pp. 1–11.

[7] L. Chen, J. Xiong, X. Chen, S. I. Lee, K. Chen, D. Han, D. Fang, Z. Tang, and Z. Wang, "Widesee: Towards wide-area contactless wireless sensing," in *Proceedings of the 17th Conference on Embedded Networked Sensor Systems*, 2019, pp. 258–270.

[8] Y. Yao, Z. Ma, and Z. Cao, "Losee: Long-range shared bike communication system based on lorawan protocol." in *EWSN*, 2019, pp. 407–412.

[9] N. Hou, X. Xia, and Y. Zheng, "Jamming of lora phy and countermeasure," in *IEEE INFOCOM 2021-IEEE Conference on Computer Communications*. IEEE, 2021.

[10] J. C. Liando, A. Gamage, A. W. Tengourtius, and M. Li, "Known and unknown facts of lora: Experiences from a large-scale measurement study," *ACM Transactions on Sensor Networks (TOSN)*, vol. 15, no. 2, pp. 1–35, 2019.

[11] A. Dongare, R. Narayanan, A. Gadre, A. Luong, A. Balanuta, S. Kumar, B. Iannucci, and A. Rowe, "Charm: exploiting geographical diversity through coherent combining in low-power wide-area networks," in *2018 17th ACM/IEEE International Conference on Information Processing in Sensor Networks (IPSN)*. IEEE, 2018, pp. 60–71.

[12] A. Gadre, R. Narayanan, A. Luong, A. Rowe, B. Iannucci, and S. Kumar, "Frequency configuration for low-power wide-area networks in a heartbeat," in *17th USENIX Symposium on Networked Systems Design and Implementation (NSDI 2020)*, 2020, pp. 339–352.

[13] Y. Lin, W. Dong, Y. Gao, and T. Gu, "Sateloc: A virtual fingerprinting approach to outdoor lora localization using satellite images," in *2020 19th ACM/IEEE International Conference on Information Processing in Sensor Networks (IPSN)*. IEEE, 2020, pp. 13–24.

[14] X. Xia and Y. Zheng, "Connecting lorawans deep inside a building," in *Proceedings of the 7th ACM International Conference on Systems for Energy-Efficient Buildings, Cities, and Transportation*, 2020, pp. 312–313.

[15] Y. Xie, Y. Zhang, J. C. Liando, and M. Li, "Swan: Stitched wi-fi antennas," in *Proceedings of the 24th Annual International Conference on Mobile Computing and Networking*, 2018, pp. 51–66.

[16] Y. Zeng, D. Wu, J. Xiong, E. Yi, R. Gao, and D. Zhang, "Farsense: Pushing the range limit of wifi-based respiration sensing with csi ratio of two antennas," *Proceedings of the ACM on Interactive, Mobile, Wearable and Ubiquitous Technologies*, vol. 3, no. 3, pp. 1–26, 2019.

[17] C. Shepard, H. Yu, N. Anand, E. Li, T. Marzetta, R. Yang, and L. Zhong, "Argos: Practical many-antenna base stations," in *Proceedings of the 18th annual international conference on Mobile computing and networking*, 2012, pp. 53–64.

[18] A. Balanuta, N. Pereira, S. Kumar, and A. Rowe, "A cloud-optimized link layer for low-power wide-area networks," in *Proceedings of the 18th International Conference on Mobile Systems, Applications, and Services (MobiSys'20)*, 2020, pp. 247–259.

[19] Gr-LoRa GitHub community. (2021, Jul) gr-lora projects. [Online]. Available: https://github.com/rpp0/gr-lora

[20] A. Hoeller, R. D. Souza, O. L. A. López, H. Alves, M. de Noronha Neto, and G. Brante, "Analysis and performance optimization of lora networks with time and antenna diversity," *IEEE Access*, vol. 6, pp. 32 820–32 829, 2018.

[21] Dragino. (2021, Mar.) Lora shield for arduino. [Online]. Available: http:// www.dragino.com/products/module/item/102-lora-shield.html

[22] L. Liu, Y. Yao, Z. Cao, and M. Zhang, "Deeplora: Learning accurate path loss model for long distance links in lpwan," in *IEEE INFOCOM 2021-IEEE Conference on Computer Communications*. IEEE, 2021.

[23] X. Wang, L. Kong, Z. Wu, L. Cheng, C. Xu, and G. Chen, "Slora: towards secure lora communications with fine-grained physical layer features," in *Proceedings of the 18th Conference on Embedded Networked Sensor Systems*, 2020, pp. 258–270.

[24] A. Gamage, J. C. Liando, C. Gu, R. Tan, and M. Li, "Lmac: Efficient carrier-sense multiple access for lora," in *The 26th Annual International Conference on Mobile Computing and Networking (MobiCom'20)*, 2020.

[25] Z. Xu, J. Luo, Z. Yin, T. He, and F. Dong, "S-mac: Achieving high scalability via adaptive scheduling in lpwan," in *IEEE INFOCOM'20*, 2020, p. 506–515.

[26] R. Eletreby, D. Zhang, S. Kumar, and O. Yagan, "Empowering low-power wide area networks in urban settings," in *Proceedings of the Conference of the ACM Special Interest Group on Data Communication*, ser. SIGCOMM'17, Aug 2017, pp. 309–321.

[27] Z. Xu, P. Xie, and J. Wang, "Pyramid: Real-time lora collision decoding with peak tracking," in *IEEE INFOCOM 2021-IEEE Conference on Computer Communications*. IEEE, 2021.

[28] Z. Xu, S. Tong, P. Xie, and J. Wang, "Fliplora: Resolving collisions with up-down quasi-orthogonality," in *2020 17th Annual IEEE International Conference on Sensing, Communication, and Networking (SECON)*. IEEE, 2020, pp. 1–9.

[29] S. Tong, Z. Xu, and J. Wang, "Colora: Enabling multi-packet reception in lora," in *IEEE INFOCOM 2020-IEEE Conference on Computer Communications*. IEEE, 2020, pp. 2303–2311.

[30] Z. Wang, L. Kong, K. Xu, L. He, K. Wu, and G. Chen, "Online concurrent transmissions at lora gateway," in *IEEE INFOCOM 2020-IEEE Conference on Computer Communications*. IEEE, 2020, pp. 2331–2340.

[31] X. Guo, L. Shangguan, Y. He, J. Zhang, H. Jiang, A. A. Siddiqi, and Y. Liu, "Aloba: rethinking on-off keying modulation for ambient lora backscatter," in *Proceedings of the 18th Conference on Embedded Networked Sensor Systems (SenSys'20)*, 2020, pp. 192–204.

[32] A. Gadre, F. Yi, A. Rowe, B. Iannucci, and S. Kumar, "Quick (and dirty) aggregate queries on low-power wans," in *2020 19th ACM/IEEE International Conference on Information Processing in Sensor Networks (IPSN)*. IEEE, 2020, pp. 277–288.

[33] H. Q. Ngo, M. Matthaiou, T. Q. Duong, and E. G. Larsson, "Uplink performance analysis of multicell mu-simo systems with zf receivers," *IEEE Transactions on Vehicular Technology*, vol. 62, no. 9, pp. 4471–4483, 2013.

[34] Q. Huang, Z. Luo, J. Zhang, W. Wang, and Q. Zhang, "Loradar: Enabling concurrent radar sensing and lora communication," *IEEE Transactions on Mobile Computing*, no. 01, nov 2020.

[35] M. Zimmerling, L. Mottola, and S. Santini, "Synchronous transmissions in low-power wireless: A survey of communication protocols and network services," *ACM Computing Surveys (CSUR)*, vol. 53, no. 6, pp. 1–39, 2020.

[36] S. Tong, J. Wang, and Y. Liu, "Combating packet collisions using non-stationary signal scaling in lpwans," in *Proceedings of the 18th International Conference on Mobile Systems, Applications, and Services*, ser. MobiSys '20, 2020, p. 234–246.

[37] X. Wang, L. Kong, L. He, and G. Chen, "mlora: A multi-packet reception protocol in lora networks," in *2019 IEEE 27th International Conference on Network Protocols (ICNP'19)*. IEEE, 2019, pp. 1–11.

[38] S. Tong, Z. Xu, and J. Wang, "Colora: Enabling multi-packet reception in lora," in *IEEE INFOCOM 2020 - IEEE Conference on Computer Communications*, 2020, pp. 2303–2311.

[39] X. Xia, N. Hou, Y. Zheng, and T. Gu, "Pcube: scaling lora concurrent transmissions with reception diversities," in *Proceedings of the 27th Annual International Conference on Mobile Computing and Networking*, 2021, pp. 670–683.